ACS APPLIED MATERIALS & INTERFACES

Research Article

www.acsami.org

# Enhancing Cubosome Functionality by Coating with a Single Layer of Poly-ε-lysine

Sonal Deshpande,[†,§,∥] Edakkal Venugopal,[†,∥] Shobha Ramagiri,[‡] Jayesh R. Bellare,[‡] Guruswamy Kumaraswamy,*[,†,∥] and Neetu Singh*[,†,§,∥]

[†]Division of Polymer Science and Engineering, National Chemical Laboratory, Dr. Homi Bhabha Road, Pune-411008, India

[∥]Academy of Scientific and Innovative Research, Rafi Marg, New Delhi-110 001, India

[§]Centre for Biomedical Engineering, Indian Institute of Technology—Delhi, Hauz Khas, New Delhi-110016, India

[‡]Chemical Engineering Department, Indian Institute of Technology—Bombay, Mumbai-400071, India

*S* *Supporting Information*

**ABSTRACT:** We report the preparation and characterization of monoolein cubosomes that can be easily surface modified through adsorption of a single layer of cationic poly-ε-lysine. Poly-ε-lysine coated cubosomes show remarkable stability in serum solution, are nontoxic and, are readily internalized by HeLa cells. The poly-ε-lysine coating provides chemical handles for further bioconjugation of the cubosome surface. We also demonstrate that the initial release rate of a hydrophilic drug, Naproxen sodium, from the cubosomes is retarded with just a single layer of polymer. Interestingly, cubosomes loaded with Naproxen sodium, recently shown to have anticancer properties, cause more apoptosis in HeLa cells when compared to free unencapsulated drug.

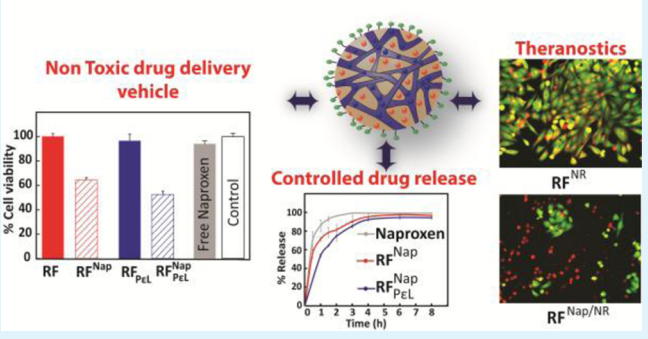


**KEYWORDS:** *bioconjugation, cubosomes, drug delivery vehicle, dual loading, theranostics*

## INTRODUCTION

Nanoparticulate drug delivery vehicles (DDVs) are platforms that can be used to overcome limitations imposed by drug solubility and stability, enhance drug circulation time and improve the ability to target particular cell types. Therefore, significant research efforts are currently focused on improved design of nanoparticulate DDVs to minimize their toxicity and to design the capability to deliver drugs in a sustained and targeted manner.[1] In particular, research has focused on multifunctional DDVs that can, for example, combine the delivery of drugs to improve patient compliance[2] or that combine multiple functionalities such as drug delivery and bioimaging.[3,4] Thus, novel DDVs that can simultaneously deliver combinations of hydrophobic and hydrophilic molecules, that can modulate the rate at which a drug is released and can be targeted to specific cells are anticipated to find numerous applications.

Nanostructures based on self-assembly of surfactant or lipid molecules represent attractive candidates for the delivery of drugs. As surfactants are amphiphilic, DDVs comprised of such molecules are able to readily solubilize hydrophobic drugs that represent a third of all new drugs.[5] Therefore, it is not surprising that liposomal DDVs have already made their way into clinics. Currently, nanoparticles of lyotropic liquid crystalline structures are being extensively investigated as DDVs because of their ability to carry hydrophobic, hydrophilic, as well as amphiphilic drugs, conventionally a major challenge for DDVs.[3,6,7] Here, we focus on an emerging class of internally nanostructured lipid particles, called cubosomes, that offer advantages relative to liposomes.[3,8] Cubosomes are self-assembled nanoparticles that are prepared from a bulk cubic phase and retain the bicontinuous microstructure of the bulk phase. Cubosomes have been reported for use as topical or subcutaneous delivery systems.[9−11] Recent reports that enhance the capabilities of cubosome based DDVs have resulted in renewed excitement about the possibilities offered by cubosomes. Driever et al.[12] have provided an important lead to address a long-standing problem with cubosomes. They have demonstrated that layer-by-layer (LbL) coating of cubosome nanoparticles by polyelectrolytes allows a moderate level of control over the initial burst release of encapsulated drug. However, the LbL protocol required the synthesis of an anchoring moiety for the polyelectrolyte chains and tedious purification procedures. Another report from the group of Murgia et al.[13] has demonstrated the preparation of drug loaded fluorescent cubosomes as theranostic probes. However, this work required the synthesis of customized fluorescent molecules. Very recently, the same group has extended this

**Received:** July 21, 2014
**Accepted:** September 3, 2014
**Published:** September 3, 2014

  

**Scheme 1. Schematic for Synthesis and Functionalization of Cubosomes**

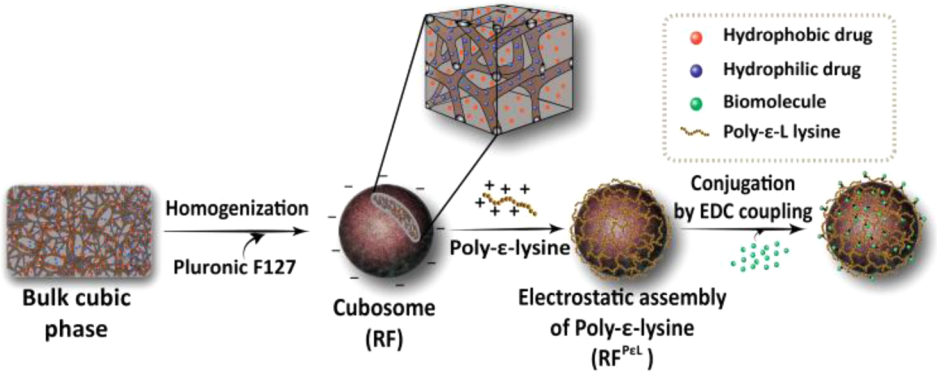


work to demonstrate theranostic cubosomes with the potential to target cancerous cells.[14] Therefore, while these reports highlight the potential of cubosomes as multifunctional DDVs, facile routes to such materials, using commercially available starting materials remain a challenge. Further, detailed studies on the interaction of cells with such multifunctional cubosome DDVs, that are essential for consideration of such materials for pharmaceutical applications, are currently unavailable.

Here, we report that coating a cubosome with a single molecular layer of poly-ε-lysine provides a route to a versatile multifunctional DDV. We describe the preparation, characterization of cubosomes that can be polymer coated and functionalized (Scheme 1). We have exploited the fact that cubosomes have a bicontinuous ordered lipid microstructure to simultaneously load both hydrophobic and hydrophilic molecules in them. We demonstrate that cubosomes have significant structural stability in biological milieu (when compared with liposomes or micelles). Coating the cubosomal surface with poly-ε-lysine not only provides chemical handles for conjugation of targeting ligands but, remarkably, allows us to decrease the burst release rate of encapsulated molecules. We present here simultaneous loading and delivery of cubosomes with hydrophilic drug naproxen sodium (NAP) and a hydrophobic dye, Nile Red (NR), which can be used for intracellular imaging. Naproxen sodium, a nonsteroidal anti-inflammatory drug (NSAID), has been recently reported to induce apoptosis of ovarian and colon cancer cells.[15,16] However, their encapsulation in a nanoparticle delivery vehicle and its efficacy has not been reported yet. We image the internalization of NAP loaded, poly-ε-lysine coated cubosomes by cells and demonstrate that these vehicles result in higher cell death.

## MATERIALS AND METHODS

**2.1. Materials.** Rylo MG 20 Pharma (henceforth called Rylo), a commercial grade monoolein-based emulsifier, was received as a generous gift from Danisco Corporation (India) and was used as received. Information from the supplier indicates that Rylo comprises predominantly glycerol monooleate (total monoglyceride> 95% with the remainder comprising di- and triglycerides and with free glycerol content <1%). We have also characterized Rylo using $^1$H NMR spectroscopy (Figure S1).

Pluronic F127 was used as obtained from BASF. Nile red was obtained from Aldrich chemicals. Naproxen sodium salt was provided by Lupin Chemicals, Pune. Poly-ε-lysine (Mw = 20 000) is obtained from CMS Chemicals Ltd. (UK). HeLa cells were obtained from National Centre for Cell Sciences, Pune, India. MTT (3-(4,5-dimethylthiazol-2-yl)-2, 5-diphenyltetrazolium bromide), fetal bovine serum (FBS), Dulbecco's phosphate buffered saline (DPBS), Dulbecco's modified eagle's medium (DMEM), 4′,6-diamidino-2-phenylindole (DAPI), calcein AM, and trypsin were obtained from Invitrogen. Dimethyl sulfoxide (DMSO) was obtained from Merck. *N*-Hydroxysuccinimide (NHS) and 5-carboxy-fluorescein diacetate *N*-succinimidyl ester were obtained from Sigma chemicals. 1-Ethyl-3-(3-(dimethylamino)propyl) carbodiimide (EDC) was obtained from Spectrochem. Dialysis tubing (12000 MWCO) was obtained from Sigma.

**2.2. Cubosome Preparation.** Cubosomes were prepared using a slight modification of a reported protocol.[17,18] Briefly, F127 Pluronic was mixed well with the Rylo melt at 80 °C to prepare a Rylo/F127 blend. The Rylo:F127 ratio was kept constant at 100:5 so as to minimize the formation of vesicles during the preparation of the cubosomes. This ratio was chosen such that the final composition is in the cubic phase region. The Rylo/F127 blend was added to deionized water and homogenized using Ultraturrax T25 from IKA at 12 000 rpm for 15 min. The milky turbid dispersion thus formed was found to be stable for more than one month. This milky dispersion was characterized using SAXS and Cryo-TEM and was observed to comprise primarily of cubosomes (that we denote RF, for Rylo/F127). We tried high pressure homogenization using an Avestin B15 homogenizer, but even relatively mild conditions (air pressure of 60 psi) resulted in the formation of a significant number density of vesicles. Therefore, we did not use high pressure homogenization for particle size reduction in this work. Cubosomes loaded with a model hydrophobic compound (Nile Red) were prepared using the same protocol but starting with a mixture of the Rylo/F127 blend with a calculated amount of Nile Red. For loading Naproxen sodium, a hydrophilic nonsteroidal anti-inflammatory drug, into the cubosomes, the following method was used. Naproxen sodium aqueous solution was prepared in deionized water and added to molten Rylo in 40:60 ratio in order to form a *Pn*3*m* cubic phase. To this *Pn*3*m* cubic phase was added an F127 solution in deionized water, such that the Rylo/F127 ratio was 100:5. This mixture was homogenized using the IKA Ultraturrax T25 to obtain cubosome dispersion. For simultaneous loading of Naproxen sodium and Nile Red, a blend of Rylo and Nile Red was prepared. Naproxen solution in deionized water was added to the molten blend of Rylo/Nile Red in the ratio of 40:60 to get a *Pn*3*m* cubic phase. The *Pn*3*m* phase was then homogenized in F127 solution in deionized water, such that the Rylo/F127 ratio is 100:5.

For preparing cubosomes coated with a biocompatible polymer, poly-ε-lysine (PεL), the following simple procedure was followed. The average size of the cubosomes is obtained using dynamic light scattering (DLS). We estimate the number density of cubosomes in solution from the DLS average size and the amount of Rylo added to water. This gives us the surface area of the cubosomes in solution. Then, we add a calculated amount of PεL solution, dropwise, to the cubosome dispersion under continuous vortexing. Particular care has been taken to add the PεL solution slowly such that the cubosomes are not phase separated. The so obtained solution has a polymer coating density of 0.5 mg/m$^2$ (designated RF$_{P\varepsilon L}$). The solution is kept for 2 days for aging and the coating of the cubosomes are confirmed by ζ potential measurement.

The nomenclature we use henceforth to represent the synthesized cubosomes is $\text{Cubosome}^{\text{Loading}}_{\text{Coating}}$. For detailed nomenclature and the samples used for different experiments refer to Table S1.

**2.3. Dynamic Light Scattering (DLS).** Size and zeta ($\zeta$) potential of the cubosomes were measured using BIC 90 Plus Particle size analyzer from Brookhaven Instruments Corporation, USA. A He−Ne laser of 632.8 nm was used and a detector at a fixed angle of 90° was employed. Data was analyzed using software supplied with the instrument to obtain the particle size distribution. The $\zeta$ potential was measured using the $\zeta$ potential analyzer attachment. Diluted and ultrasonicated (for about 20 min) samples were used to avoid multiple scattering. All measurements were done in triplicate and the standard deviations were plotted as error bars.

**2.4. Small Angle X-ray Scattering (SAXS).** The SAXS experiments were done on a Bruker Nanostar equipped with a rotating anode and three pinhole collimation. The instrument uses Cu−K$\alpha$ radiation of wavelength 1.54 Å and a sample to detector length of about 105 cm. The anode was operated at 45 kV and 100 mA current. The samples were taken in a 2 mm quartz capillary (from Charles-Supper, USA) with 10 $\mu$m wall thickness. Scattering from glassy carbon film was used as the reference. A Peltier unit was used for controlling the temperature of the sample holder. The data was collected on a HISTAR gas filled multiwire detector and the 2D data was circularly averaged to reduce the data to 1D. Samples were scanned sufficiently long to get at least two million counts and were normalized with the transmission coefficient of the sample and the acquisition time. The detector was calibrated using the scattering from silver behenate.

**2.5. Cryo-TEM.** Samples were prepared for Cryo-TEM by the frozen hydrated vitrified technique[19] using a Vitrobot Mark IV semiautomated sample preparation system. About 3 $\mu$L of liquid sample was taken on a lacey fomvar carbon coated 200 mesh copper grid kept in an environmental chamber at a temperature 22 °C and humidity 85%. The sample was made into a thin film by blotting once for one second with a blot force setting of one, and then plunged into liquid ethane at its freezing point. The resultant vitrified grid was transferred under liquid nitrogen to a Gatan model 655 cryo holder with a cryo-transfer system, and then cryo-transferred into the TEM goniometer while maintaining the cold chain throughout. Imaging was done in a JEOL 2100 HRTEM operating at 200 keV while maintaining the sample holder at about −172.6 °C as measured by a Gatan Smartset model 900 cold stage controller.

**2.6. Serum Stability Test.** Dispersion of the cubosomes in serum could lead to adsorption of proteins and to changes in the cubosome structure, and the cubosome could eventually disintegrate. To check the stability of the cubosome in biologically relevant media, we monitored changes in the size of RF and $\text{RF}_{\text{P}\epsilon\text{L}}$ with time using DLS. Both coated and uncoated cubosomes were incubated at a fixed concentration with 10% FBS and their particle size was measured at different time intervals. DLS was performed at a fixed angle of 90° and the scattering counts were analyzed. All experiments were done in triplicate and the standard deviations among the experiments were plotted as error bars.

**2.7. Cytotoxicity Assay.** Cytotoxicity of cubosomes was evaluated using MTT assay. Cells were cultured in DMEM (high glucose) supplemented with 10% FBS under 5% $CO_2$ at 37 °C. They were seeded in a 96 well plate in 200 $\mu$L media at a seeding density of 10 000 cells/well. Cubosomes were UV sterilized for 1 h. After overnight incubation of the seeded cells, media was replaced with 200 $\mu$L cubosomes (dispersed in DMEM) of various concentrations. The cubosomes were added in triplicate and incubated for 24 h. After 24 h of culture, media was removed and cells were washed with DPBS. MTT (0.5 mg/mL) in DMEM was added to the wells and incubated for another hour (until the formation of purple formazan crystals in control wells). The media was removed and the formazan crystals were solubilized in 200 $\mu$L DMSO. Absorbance was recorded at 550 nm using iMarkMicroplate Absorbance Reader (BIORAD). The data was plotted with standard deviation (from three sets of independent experiments) as error bars. Same protocol was followed for evaluating cytotoxicity of naproxen loaded cubosomes. A student's $t$-test was performed for analyzing statistical significance.

**2.8. Cellular Uptake.** The cellular uptake of the cubosomes was first analyzed by fluorescence microscopy. Circular coverslips (12 mm in diameter) were kept overnight in absolute ethanol for sterilization. They were then placed in a 24 well plate and washed three times with DPBS to remove traces of ethanol. Cells were seeded in 1 mL cell culture media at density of $3 \times 10^4$ cells/well and incubated overnight. Media was replaced with Nile Red loaded cubosomes (0.08 mg/mL) in media and then incubated for another 4 h. After incubation, the medium was removed and cells were washed three times with DPBS. Cells were then washed once with 0.05% Tween20 followed by three washes with DPBS. Cells were fixed with 300 $\mu$L 4% (w/v) paraformaldehyde for 15 min, followed by three washes with DPBS. For counterstaining nuclei, 300 nM DAPI was added to the cells for 30 s, washed three times with DPBS and observed under Carl Ziess fluorescence microscope using DAPI and rhodamine filters.

Uptake was also quantified by flow cytometry. Cells were seeded in a 6 well plate in 4 mL media at a density of $3 \times 10^5$ cells/well and incubated overnight. Media was replaced with culture media containing 0.06 mg/mL of Nile Red loaded cubosomes and incubated for another 4 h. Cells were washed with 0.05% Tween20 followed by the treatment with trypsin for 3 min. The cell suspension was centrifuged at 2000 rpm for 5 min, resuspended in sterile DPBS containing 10% FBS and passed through a BD Falcon 40 $\mu$m cell strainer. Uptake was monitored using PE filter using a BD Canto FACS machine.

**2.9. Conjugation of Fluorescein on Coated Cubosomes.** Poly-$\epsilon$-lysine coated cubosomes were diluted to 25 mg/mL in DPBS, and 10 $\mu$L of fluorescein−NHS (2 mg/mL) was added to it. The reaction was carried at room temperature for 2 h. The reaction mixture was dialyzed using 3.5 kDa dialysis tubing overnight to remove unreacted fluorescein. A similar protocol was used for poly-$\epsilon$-lysine coated cubosomes loaded with Nile Red. Conjugation was confirmed by recording absorbance spectra of the samples using a Cary50 UV−vis spectrophotometer.

**2.10. Release of Naproxen Sodium from Cubosomes.** Release of Naproxen sodium was studied using equilibrium dialysis. Naproxen-loaded-coated cubosomes ($\text{RF}^{\text{Nap}}_{\text{P}\epsilon\text{L}}$), Naproxen-loaded-uncoated cubosomes ($\text{RF}^{\text{Nap}}$), and free Naproxen sodium solution were dialyzed using 12 kDa dialysis membrane. At each time point ($t$) a 50 $\mu$L sample was aliquoted and added to 650 $\mu$L DMSO, in order to dissolve the cubosomes. The absorbance of naproxen sodium left was monitored at 330 nm using Cary50 UV−vis spectrophotometer. Percent release was calculated using following formula:

$$\%\ \text{release} = 100 - \left(\frac{\text{absorbance at time "}t\text{"}}{\text{absorbance at time zero}} \times 100\right)$$

**2.11. Cubosomes as Theranostic Probes.** HeLa cells were plated in a 24 well plate at seeding density of $3 \times 10^4$ cells/well and incubated overnight. After the overnight incubation, UV sterilized $\text{RF}^{\text{Nap}}$ and $\text{RF}^{\text{Nap/NR}}$ cubosomes (diluted to 0.1 mg/mL in media) were added over the cells. The $\text{RF}^{\text{Nap}}$ cubosomes were used as control. After 24 h of incubation, cells were stained with calcein AM for 15 min and imaged under FLoid Cell Imaging Station using red and green filters.

## RESULTS AND DISSCUSSION

**3.1. Characterization and Surface Coating of Cubosomes.** Rylo/F127 mixtures form liquid crystalline mesophases that were characterized using small-angle X-ray scattering (SAXS, Figure 1a). For the Rylo/F127 bulk phase (BP, Figure 1a), we observed SAXS peaks characteristic of a double diamond cubic phase characterized by space group $Pn3m$, with a lattice parameter of 103.2 Å.[17,18] On homogenizing BP, we obtain a turbid, milky dispersion that we term RF. RF was characterized using Cryo-TEM and SAXS. Cubic mesophases of glycerol monooleate scatter X-rays poorly, necessitating long acquisition times Therefore, for low concentration RF

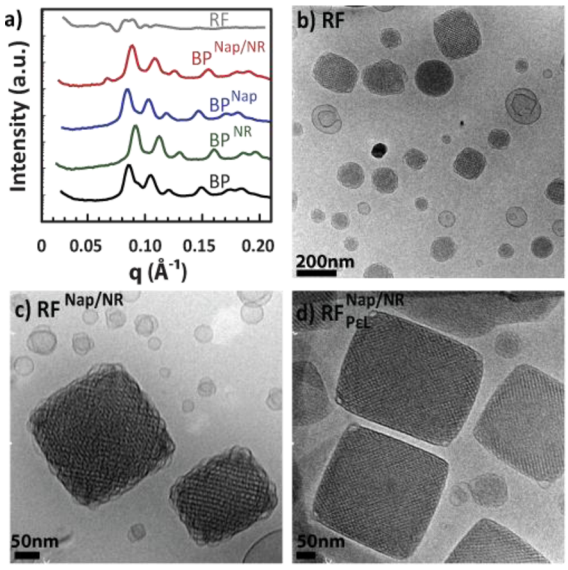


**Figure 1.** (a) SAXS pattern for the cubosomes and the bulk phase (BP) before and after loading with hydrophobic (nile red) and hydrophilic (naproxen) molecules: ($BP^{NR}$) BP loaded with Nile Red, ($BP^{Nap}$) BP loaded with Naproxen sodium, ($BP^{Nap/NR}$) BP loaded with Nile Red and Naproxen sodium. Cryo-TEM for (b) cubosomes (RF), (c) Naproxen and Nile Red loaded cubosomes ($RF^{Nap/NR}$), and (d) Naproxen and Nile Red loaded, coated cubosomes ($RF^{Nap/NR}_{P\varepsilon L}$).

dispersions, the SAXS data is noisy. However, the locations of the first two peaks (around 0.08 and 0.11 $Å^{-1}$, Figure 1a) are similar to those for BP and suggest that the *Pn*3*m* cubic phase structure is retained in RF. The RF also shows the presence of other peaks (for example, around 0.06 $Å^{-1}$), indicating that a small fraction of other mesophases might also be present. We estimate an apparent cubic phase lattice parameter (≈107 Å) for the RF dispersion, higher than for BP. We term the lattice parameter as "apparent" due to uncertainties in determining the peak positions due to poor scattering from RF dispersions, combined with the presence of other phases. Confirmation for the cubic phase internal organization in the RF particles comes from Cryo-TEM (Figure 1b). The RF dispersion comprises polydisperse particles that are smaller than about 200 nm (Figure S2a). In the Cryo-TEM images, RF particles exhibit a faceted shape, characteristic of cubosomes and, show evidence for internal organized microstructure. We also observed the coexistence of vesicles. These are known to form[20] when high speed homogenization is used for cubosome synthesis. In protocols typically reported in the literature, the homogenization step is followed by prolonged heat treatment to eliminate vesicular structures.[21] However, since several drugs are temperature- sensitive, our synthesis protocol does not employ heating. Even without the heat treatment, we observe that the RF sample contains predominantly cubosomes, with only a small fraction of vesicles.

The *Pn*3*m* cubic phase is retained even on loading the Rylo/F127 bulk phase with a hydrophilic drug (Naproxen Na, up to a loading of 1% by weight (Figure 1a and Figure S2b) or, hydrophobic molecule, Nile Red, up to a loading of 0.05% by weight (Figure 1a and Figure S2c) or with a combination of hydrophilic drug (Naproxen Na) and hydrophobic dye (Nile Red). Incorporation of the hydrophobic dye decreases the lattice parameter to 101.4 Å, while loading of hydrophilic Naproxen Na results in an increase to 105.5 Å (relative to 103.2 Å, observed for BP). Remarkably, there is very little change in the lattice parameter relative to BP on simultaneous loading of Nile Red and Naproxen Na (103.6 Å for $BP^{Nap/NR}$, Figure 1a).

Incorporation of hydrophobic or hydrophilic moieties can change the critical packing parameter (CPP) associated with the lipid[22] resulting in dramatic changes in mesophase organization.[23−25] For example, a recent report[13] indicates the formation of "rose" like particles on incorporation of a hydrophobic molecule in a Rylo/water phase. However, for loadings of up to 1% of Naproxen Na, or 0.05% of Nile Red, we observe that the *Pn*3*m* phase is retained in the Rylo/water system. Cryo-TEM confirms that homogenization of $BP^{Nap/NR}$ (to form $RF^{Nap/NR}$ dispersions) results in the formation of faceted internal cubic phase dispersed particles, similar to those observed for RF dispersions (Figure 1c). As in the case of RF, we observe a few vesicle structures and note the formation of lamellar phases at the outer surface of the $RF^{Nap/NR}$ that we attribute to F127 surface layers, in accord with the literature.

The change in the lattice parameter in the cubic phase can be rationalized by considering how the incorporated moieties are localized in the mesophase.[22] Hydrophilic molecules are localized in the water channels and increase the effective hydrophilic headgroup area of the lipids.[22,23,26] We observe that this is associated with an increased lattice parameter. Conversely, when hydrophobic molecules are loaded in the cubosomes, these molecules are likely to be localized near the lipid tails. This is associated with a decrease in lattice parameter. For the simultaneous loading of hydrophilic and hydrophobic molecules, the lattice parameter remains essentially unchanged. We note that $BP^{Nap/NR}$ is a four-component system and is likely to manifest complex phase behavior. Therefore, the fact that $BP^{Nap/NR}$ exhibits a cubic phase with a similar lattice parameter to BP is fortuitous.

Decoration of the cubosome surface with oligo-ethylene oxide segments from the F127 is considered to confer the advantage of increased circulation times in the body, similar to that for "stealth" liposomes.[27] However, F127 is chemically inert and is not amenable to chemical conjugation, precluding surface functionalization of cubosomes. Therefore, we electrostatically coupled RF cubosomes with a cationic natural homopolymer, poly-ε-lysine (PεL). RF cubosomes are negatively charged, and exhibit a zeta potential of −24 ± 7 mV (Figure S2a). The origin of the negative zeta potential for cubosomes has been attributed to the adsorption of hydroxyl ions at the cubosome surface.[28] Commercially available Rylo that was used to prepare cubosomes in our work also contains some free oleic acid, that too might also contribute to the observed zeta potential. PεL coated cubosomes, termed, $RF_{P\varepsilon L}$, exhibit a size (by DLS) of 200 ± 39 nm, slightly larger than RF (DLS size of 165 ± 25 nm, (Figure S2a)). The zeta potential after coating changes from about −24 ± 7 to +2 ± 1 mV, providing evidence for the complexation of PεL with the cubosome surface (Figure S2a). Cryo-TEM of $RF^{Nap/NR}_{P\varepsilon L}$ confirms that the PεL coating does not alter the cubic phase internal structure of the cubosomes (Figure 1d).

Recently, layer-by-layer (LbL) coating of cubosomes using electrostatic complexation of alternating layers of polymethacrylic acid and poly-L-lysine has been reported by the group of Caruso and Drummond.[12] In their work, the first layer on the cubosome surface was hydrophobically anchored through a specially synthesized anionic copolymer containing a hydrophobic "anchoring" moiety. They reported that this strategy of using a strongly anchored polyanion on the cubosome surface

was essential for multilayer formation. They claim that complexation of polycations with hydroxyl ions adsorbed on the cubosome surface could not sustain multilayer formation. Further, LbL on the cubosome surface necessitated separation of free polyanion-polycation complexes using centrifugation. They reported that release of a model hydrophilic compound, fluorescein, was modulated for cubosomes coated with seven polymer layers, with a moderate decrease in the initial burst release, relative to uncoated F127 stabilized cubosomes.

In our work, we deposit only a single layer of PεL on the cubosome surface. A calculated amount of PεL is added to the cubosome layer (as detailed in the Materials and Methods section), such that a surface coating of about 0.5 mg/m$^2$ is obtained (comparable to literature estimates of the surface coverage obtained by electrostatic polyelectrolyte complexation). We observe that the PεL coated cubosomes thus obtained are stable in solution and do not aggregate over several days. While the zeta potential for PεL-coated cubosomes (Figure S2a) is only marginally positive, this compares well with that obtained by Driever et al.[12] for cubosomes coated with a single layer of polycation. Our strategy has the significant advantage that it involves no separation steps. Remarkably, our data indicates that even this single layer of PεL is able to influence the initial burst release of hydrophilic Naproxen Na from loaded cubosomes. We now present data that compares the release of Naproxen Na from $RF^{Nap}$ and $RF^{Nap}_{P\varepsilon L}$

**3.2. Naproxen Release from Cubosomes.** We investigated the release of NAP via dialysis. While Boyd[29] has raised concerns about the use of dialysis to determine the release rate from cubosomes, Driever et al.[12] suggest that these concerns can be overcome by the use of dialysis tubing with a molecular weight cutoff that is significantly larger than the size of the released molecule. Following Driever et al.[12] we adopt the dialysis method and use dialysis tubing with a cutoff that is over 60 fold larger than the molecular weight of NAP. Before the release experiment, dialysis tubes were boiled for 30 min and then washed thoroughly to remove impurities. The control, unencapsulated NAP, is released rapidly with 70 ± 9% release within the first 30 min, 85 ± 6% within an hour and almost 100% released within the first 3 h (Figure 2a). The rate of release of NAP is similar to that of fluorescein (Figure S3) and is slower than that reported in similar experiments.[12] These might arise due to subtle differences in the experimental setup. Here, we compare release of the NAP relative to the unencapsulated NAP control. Thus, changes in release rates can be attributed to the additional diffusion resistance introduced by encapsulating NAP in the cubosomes. In comparison to the control, the initial burst release of NAP from the RF cubosomes was lower (~55 ± 4% in the first 30 min, ~70 ± 2% in an hour and complete release over about 6 h). For the PεL coated cubosomes ($RF^{Nap}_{P\varepsilon L}$), the burst release is retarded even more significantly with just over 53 ± 2% of the loaded NAP released in the first hour, ~64 ± 1% release over 2 h and complete release over 6−8 h (Figure 2a). Similar release profiles were observed for the release of NAP from the $RF^{Nap}$ and $RF^{Nap}_{P\varepsilon L}$ cubosomes in 10% serum (Figure S4).

Thus, it appears that coating the cubosomes even with a single layer of PεL is effective in retarding the initial burst release of NAP. Since NAP is negatively charged it can electrostatically interact with PεL and we believe that this results in a slower release. The data clearly indicates the ability to tune the release profile of NAP by the PεL coating.

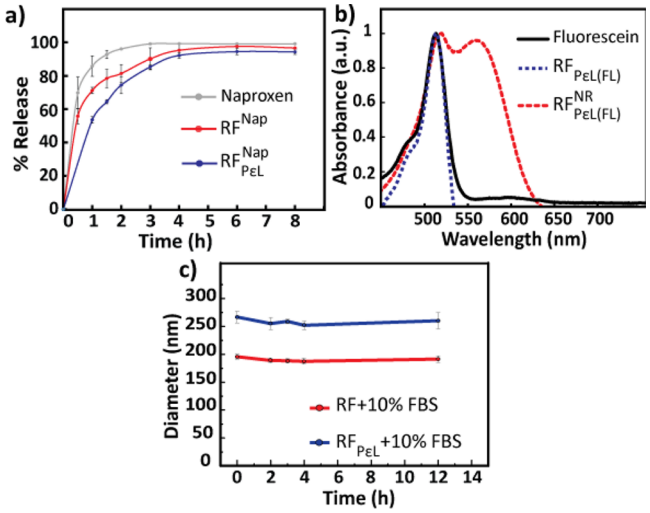


**Figure 2.** (a) Release profile of Naproxen when unencapsulated (gray) and loaded in $RF^{Nap}$ (red) and $RF^{Nap}_{P\varepsilon L}$ (blue) cubosomes. (b) Absorbance spectra for $RF_{P\varepsilon L}$ (blue) and NR-loaded-coated cubosomes, $RF^{NR}_{P\varepsilon L}$ (red) after conjugation with fluorescein (FL). (c) Size changes over time of RF (red) and $RF_{P\varepsilon L}$ (blue) after incubating in 10% FBS monitored by DLS.

Interestingly, simultaneous loading of cubosomes with NAP and Nile Red ($RF^{Nap/NR}$) further retards the release of NAP relative to $RF^{Nap}$ (Figure S5). We observed that after 2 h, while 80 ± 5% NAP was released from $RF^{Nap}$, only 68 ± 6% NAP was released from $RF^{Nap/NR}$. We believe that the retardation of NAP release from NAP/NR loaded cubosomes could be due to the aromatic group interaction of the drug and the dye.

**3.3. Surface Conjugation.** To investigate if the primary amines on PεL can be utilized for further bioconjugation with a targeting moiety, we conjugated fluorescein to the surface of $RF^{NR}_{P\varepsilon L}$ via carbodiimide coupling. Conjugation of fluorescein was confirmed by UV−vis absorption spectra of the cubosomes (Figure 2b). Murgia et al.[13] have commented on the difficulty in dispersing fluorescein in monoolein cubosomes. The conjugation strategy that we describe demonstrates a facile route to incorporation of fluorescein at the cubosome surface. We note that our strategy is not limited to incorporation of fluorescein but can be readily extended to a wide variety of functional moieties and, can be extended for developing drug delivery vehicles that exhibit targeting moieties on their surfaces. Fluorescein conjugation does not perturb the encapsulated hydrophobic compound: the absorption spectrum of surface conjugated NR-loaded cubosomes ($RF^{NR}_{P\varepsilon L}$) exhibits peaks at $\lambda_{max}$ = 565 and 515 nm (corresponding to Nile Red and fluorescein respectively, Figure 2b) indicating the simultaneous presence of both dyes. Conjugation also does not result in aggregation or degradation of the cubosomes as no significant change was observed in the size of the cubosomes (Figure S6a).The surface modification of cubosomes with fluorescein was also confirmed by fluorescence microscopy. An outer green ring was observed when fluorescein-conjugated-NR-loaded cubosomes were imaged (Figure S6b).

**3.4. Drug Delivery and Theranostic Applications of Cubosomes.** After characterizing the size and the internal microstructure of the cubosomes, we explored the possibility of using uncoated (RF) and coated cubosomes ($RF_{P\varepsilon L}$) for drug delivery applications. We first tested their aggregation and structural stability in a biologically relevant solution. Interaction

with serum albumin is known to destabilize the nanoparticle structure and lead to premature drug release and aggregation.[30,31] We monitored the changes in the cubosome size over time when incubated in 10% fetal bovine serum solution. For both RF and $RF_{P\varepsilon L}$, we observe no significant change in size with time, suggesting that the cubosomes are stable against aggregation due to serum for 12 h (Figure 2c). P$\varepsilon$L coating does not affect the stability of cubosomes in serum.

We next studied the cellular interaction of the coated and uncoated cubosomes by evaluating their cytotoxicity and cellular uptake. The cytotoxicity of RF and $RF_{P\varepsilon L}$ on HeLa cells was determined by tetrazolium (MTT) assay, a colorimetric assay for cellular viability. We observed that both coated and uncoated cubosomes were nontoxic and well tolerated by HeLa cells and almost 100% cell viability was maintained up to 0.1 mg/mL (Figure 3a). Thus, these results confirm the biocompatibility of both P$\varepsilon$L coated and uncoated cubosomes.

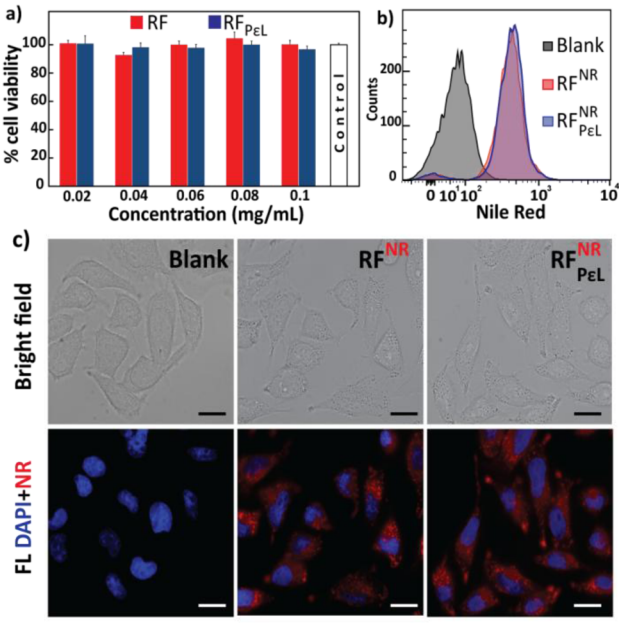


**Figure 3.** (a) Viability of HeLa cells after incubation with uncoated (RF) and coated ($RF_{P\varepsilon L}$) cubosomes (assayed by MTT). The error bar is standard error from three independent experiments done in triplicate. (b) Cellular uptake of Nile Red (NR) loaded cubosomes indicated by the shift in NR fluorescence intensity for the cell count due to the uptake of $RF^{NR}$ (red) and $RF^{NR}_{P\varepsilon L}$ (blue) compared to the control (gray). (c) Cellular uptake of NR loaded cubosomes observed by fluorescence microscopy. DAPI was used for counterstaining nucleus. Imaging was done at 63× magnification: (blue) DAPI, (red) cubosomes. Scale bar = 20 $\mu$m.

We investigated the cellular uptake of the NR loaded, uncoated and P$\varepsilon$L coated cubosomes, by incubating them with HeLa cells for 4 h, followed by analysis using flow cytometery (Figure 3b) and fluorescence microscopy (Figure 3c). The presence of Nile Red in the cubosomes enables their easy intracellular detection. To quantify the efficiency of cellular uptake we first analyzed the cells by flow cytometry. Both, uncoated and P$\varepsilon$L coated cubosomes were efficiently internalized by cells, since almost the entire population of cells had red fluorescence. This is clearly indicated by the histograms for cell population vs Nile Red fluorescence in Figure 3b. There is a large shift in Nile Red fluorescence intensity for the $RF^{NR}$ (red histogram) and $RF^{NR}_{P\varepsilon L}$ (blue histogram) in comparison to the controls (gray histogram, which represent cells that were not incubated with cubosomes). Interestingly, no significant difference was observed in the internalization of $RF^{NR}$ and $RF^{NR}_{P\varepsilon L}$ cubosomes, even though the surface charges are different. We also confirmed the cellular internalization of cubosomes by fluorescence and confocal microscopy. As can be seen in Figure 3c cells incubated with NR loaded cubosomes (coated and uncoated) showed strong red fluorescence due to intracellular localization, suggesting good cellular uptake. Analysis by confocal microscopy confirmed that the cubosomes were internalized and not present on the cell surface (Figure S7) as most of the cubosomes were observed between 15 and 30 $\mu$m in $z$ axis scans.

After confirming the cellular biocompatibility and uptake of NR-loaded, coated and uncoated cubosomes, we investigated the use of NR/NAP loaded cubosomes as dual function theranostic probes. We first checked the efficacy of uncoated and P$\varepsilon$L coated NAP-loaded cubosomes in HeLa cells by assessing cell viability. After 24 h of incubation with HeLa cells, concentration dependent cell death was observed (Figure 4a and Figure S8). We used various concentrations of unloaded cubosomes and free NAP as controls and observed almost 100% cell viability at all concentrations. The uncoated-NAP-loaded ($RF^{Nap}$) cubosomes showed about 60% cell viability compared to the P$\varepsilon$L-coated-NAP-loaded ($RF^{Nap}_{P\varepsilon L}$) cubosomes, which showed 50% cell viability at the highest NAP concentration (1 $\mu$g/mL). Since the internalization of cubosomes appears to be largely unaffected by P$\varepsilon$L-coating (Figure 3c), we attribute the higher cell death observed for P$\varepsilon$L-coated cubosomes to their ability to retain and deliver NAP more efficiently to the cells. Our NAP release data, indicating a retardation of the burst release on coating with P$\varepsilon$L is consistent with this explanation. An intriguing result was the improved efficacy of NAP when encapsulated in cubosomes, when compared with the un- encapsulated (free) drug. Such enhancement in drug efficiency on encapsulation has been observed in other lipid based drug delivery vehicles and has been attributed to better cellular internalization and protection from degradation of the drug,[32−34] due to the encapsulation. The detailed mechanism of action of this improved efficacy is beyond the scope of this paper and is currently being investigated in our laboratory.

To confirm that the cell death was due to internalization of cubosomes loaded with NAP, we imaged the cells after incubating with the dual loaded (NR and NAP) cubosomes. The live cells were stained with calcien AM, a dye that fluoresces green after intracellular cleavage by esterases. The dead cells, indicated by the rounded cellular morphology, fluoresced red (due to NR) clearly indicating the internalization of $RF^{Nap/NR}$ cubosomes (Figure 4b and Figure S9). As evident from the bright field and the fluorescence images, cubosomes loaded with NAP induced cell death very efficiently when compared with cubosomes without NAP. Interestingly, for $RF^{Nap/NR}$ some live cells also fluoresced red suggesting that the cubosomes are internalized but apoptosis has not occurred. This is in accordance with the 60% cell viability observed by the MTT assay. These results indicate the versatility of the cubosome vehicles, and their potential for use as theranostic platforms that allow simultaneous delivery of therapeutics and imaging.

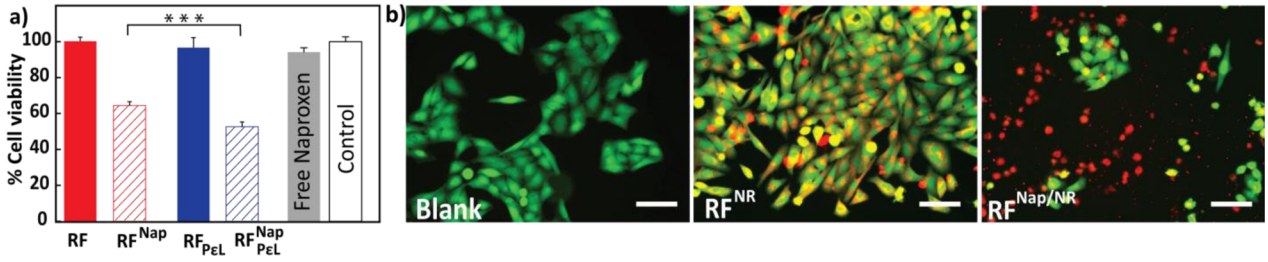


**Figure 4.** (a) Viability of HeLa cells after incubating with Naproxen-loaded uncoated ($RF^{Nap}$) and coated ($RF^{Nap}_{P\varepsilon L}$) cubosomes for 24 h. The error bar is standard error of three independent experiments performed in triplicate. Statistical significance is indicated by *** ($P < 0.001$). (b) Images of HeLa cells after incubation with Nile Red (NR) and Naproxen (Nap) loaded cubosomes. The live cells were stained with calcein AM. Red represents fluorescence due to NR. Imaging was done at 20× magnification: (green) calcein AM, (red) cubosomes. Scale bar = 100 $\mu$m.

## CONCULSIONS

We demonstrate that cubosomes with internal *Pn3m* structure, prepared with monoolein, can be transformed into multifunctional nanoparticles by coating them with a single layer of biocompatible polymer, poly-$\varepsilon$-lysine (P$\varepsilon$L). P$\varepsilon$L-coated cubosomes are nontoxic and are readily internalized by cells. Even the single layer of P$\varepsilon$L is able to retard the burst release of hydrophilic drugs, such as Naproxen Na (NAP), encapsulated in cubosomes. Coated cubosomes afford facile chemical conjugation of their surfaces, while retaining their internal microstructure. We demonstrate that theranostic devices can be prepared by simultaneous loading of cubosomes with a hydrophobic dye, Nile Red (NR), and a drug, NAP. P$\varepsilon$L-coated NAP/NR loaded cubosomes were observed to lead to efficient cell death, even when compared with free NAP. The NAP/NR loaded theranostic devices allowed spatial monitoring of drug internalization by cells and their correlation with cell death.

## ASSOCIATED CONTENT

### Supporting Information

Figures S1−S9 as mentioned in the text. Proton NMR of Rylo, nomenclature of cubosomes, characterization by DLS and zeta, characterization of naproxen and Nile Red loading, release profiles, surface conjugation by imaging, confocal images for cubosome uptake, cell viability for $RF^{Nap}$ and $RF^{Nap}_{P\varepsilon L}$, cell morphology after incubation with $RF^{Nap/NR}$. This material is available free of charge via the Internet at http://pubs.acs.org.

## AUTHOR INFORMATION

### Corresponding Authors

*E-mail: g.kumaraswamy@ncl.res.in. Fax: + 91-20-2590-2168. Tel.: + 91-20-25902182 (G.K.).

*E-mail: sneetu@iitd.ac.in. Fax: + 91-11-26582037. Tel.: + 91-011-26591422 (N.S.).

### Notes

The authors declare no competing financial interest.

## ACKNOWLEDGMENTS

We acknowledge financial support from CSIR-NCL and CSIR network project M2D. G.K. acknowledges funding from the DST through the Chemical Engineering PAC. N.S. acknowledges funding from DST-Nanomission and IYBA (DBT). S.D. and E.V. acknowledge fellowship support from UGC and CSIR, respectively. We thank Gaurav Chaudhry from Danisco for supplying us Rylo. We thank IIT Bombay for use of Cryo-TEM Central Facilities funded by DST and DBT. We acknowledge help from Manoj Kumar in optimizing the protocol for preparation of the cubosomes. We also acknowledge Dr. Sharvil Patil from the Poona College of Pharamcy for providing us a sample of Naproxen sodium.

## ABBREVIATIONS

P$\varepsilon$L, poly-$\varepsilon$-lysine
RF, Rylo-Pluronic F127 cubosomes
$RF^{Nap}$, Naproxen loaded cubosomes
$RF^{Nap}_{P\varepsilon L}$, Naproxen loaded P$\varepsilon$L coated cubosomes
$RF^{NR}$, Nile Red loaded cubosomes
$RF^{NR}_{P\varepsilon L}$, Nile Red loaded P$\varepsilon$L coated cubosomes
$RF^{Nap/NR}$, Naproxen and Nile Red loaded cubosomes
$RF^{Nap/NR}_{P\varepsilon L}$, Naproxen and Nile Red loaded P$\varepsilon$L coated cubosomes

## REFERENCES

(1) Couvreur, P. Nanoparticles in Drug Delivery: Past, Present and Future. *Adv. Drug Delivery Rev.* **2013**, *65*, 21−23.

(2) Pandey, R.; Zahoor, A.; Sharma, S.; Khuller, G. Nanoparticle Encapsulated Antitubercular Drugs as a Potential Oral Drug Delivery System against Murine Tuberculosis. *Tuberculosis* **2003**, *83*, 373−378.

(3) Mulet, X.; Boyd, B. J.; Drummond, C. J. Advances in Drug Delivery and Medical Imaging Using Colloidal Lyotropic Liquid Crystalline Dispersions. *J. Colloid Interface Sci.* **2013**, *393*, 1−20.

(4) Xie, J.; Lee, S.; Chen, X. Nanoparticle-Based Theranostic Agents. *Adv. Drug Delivery Rev.* **2010**, *62*, 1064−1079.

(5) Kim, S.; Shi, Y.; Kim, J. Y.; Park, K.; Cheng, J.-X. Overcoming the Barriers in Micellar Drug Delivery: Loading Efficiency, *in Vivo* Stability, and Micelle−cell Interaction. *Expert Opin. Drug Delivery.* **2010**, *7*, 49−62.

(6) Pan, X.; Han, K.; Peng, X.; Yang, Z.; Qin, L.; Zhu, C.; Huang, X.; Shi, X.; Dian, L.; Lu, M.; Wu, C. Nanostructured Cubosomes as Advanced Drug Delivery System. *Curr. Pharm. Des.* **2013**, *19*, 6290−6297.

(7) Guo, C.; Wang, J.; Cao, F.; Lee, R. J.; Zhai, G. Lyotropic Liquid Crystal Systems in Drug Delivery. *Drug Discovery Today* **2010**, *15*, 1032−1040.

(8) Yaghmur, A.; Glatter, O. Characterization and Potential Applications of Nanostructured Aqueous Dispersions. *Adv. Colloid Interface Sci.* **2009**, *147−148*, 333−342.

(9) Bender, J.; Ericson, M. B.; Merclin, N.; Iani, V.; Rosén, A.; Engström, S.; Moan, J. Lipid Cubic Phases for Improved Topical Drug Delivery in Photodynamic Therapy. *J. Controlled Release* **2005**, *106*, 350−360.

(10) Lopes, L. B.; Lopes, J. L. C.; Oliveira, D. C. R.; Thomazini, J. A.; Garcia, M. T. J.; Fantini, M. C. A.; Collett, J. H.; Bentley, M. V. L. B. Liquid Crystalline Phases of Monoolein and Water for Topical Delivery of Cyclosporin A: Characterization and Study of in Vitro and in Vivo Delivery. *Eur. J. Pharm. Biopharm.* **2006**, *63*, 146−155.

(11) Fong, W.-K.; Hanley, T.; Boyd, B. J. Stimuli Responsive Liquid Crystals Provide "on-Demand" Drug Delivery in Vitro and in Vivo. *J. Controlled Release* **2009**, *135*, 218−226.

(12) Driever, C. D.; Mulet, X.; Waddington, L. J.; Postma, A.; Thissen, H.; Caruso, F.; Drummond, C. J. Layer-by-Layer Polymer Coating on Discrete Particles of Cubic Lyotropic Liquid Crystalline Dispersions (Cubosomes). *Langmuir* **2013**, *29*, 12891−12900.
(13) Murgia, S.; Bonacchi, S.; Falchi, A. M.; Lampis, S.; Lippolis, V.; Meli, V.; Monduzzi, M.; Prodi, L.; Schmidt, J.; Talmon, Y.; Caltagirone, C. Drug-Loaded Fluorescent Cubosomes: Versatile Nanoparticles for Potential Theranostic Applications. *Langmuir* **2013**, *29*, 6673−6679.
(14) Caltagirone, C.; Falchi, A. M.; Lampis, S.; Lippolis, V.; Meli, V.; Monduzzi, M.; Prodi, L.; Schmidt, J.; Sgarzi, M.; Talmon, Y.; Bizzarri, R.; Murgia, S. Cancer-Cell-Targeted Theranostic Cubosomes. *Langmuir* **2014**, *30*, 6228−6236.
(15) Zerbini, L. F.; Tamura, R. E.; Correa, R. G.; Czibere, A.; Cordeiro, J.; Bhasin, M.; Simabuco, F. M.; Wang, Y.; Gu, X.; Li, L.; Sarkar, D.; Zhou, J.-R.; Fisher, P. B.; Libermann, T. A. Combinatorial Effect of Non-Steroidal Anti-Inflammatory Drugs and NF-κB Inhibitors in Ovarian Cancer Therapy. *PLoS One* **2011**, *6*, e24285.
(16) Suh, N.; Reddy, B. S.; DeCastro, A.; Paul, S.; Lee, H. J.; Smolarek, A. K.; So, J. Y.; Simi, B.; Wang, C. X.; Janakiram, N. B.; Steele, V.; Rao, C. V. Combination of Atorvastatin with Sulindac or Naproxen Profoundly Inhibits Colonic Adenocarcinomas by Suppressing the p65/ -Catenin/Cyclin D1 Signaling Pathway in Rats. *Cancer Prev. Res. (Phila. Pa.)* **2011**, *4*, 1895−1902.
(17) Gustafsson, J.; Ljusberg-Wahren, H.; Almgren, M.; Larsson, K. Cubic Lipid−Water Phase Dispersed into Submicron Particles. *Langmuir* **1996**, *12*, 4611−4613.
(18) Gustafsson, J.; Ljusberg-Wahren, H.; Almgren, M.; Larsson, K. Submicron Particles of Reversed Lipid Phases in Water Stabilized by a Nonionic Amphiphilic Polymer. *Langmuir* **1997**, *13*, 6964−6971.
(19) Bellare, J. R.; Davis, H. T.; Scriven, L. E.; Talmon, Y. Controlled Environment Vitrification System: An Improved Sample Preparation Technique. *J. Electron Microsc. Tech.* **1988**, *10*, 87−111.
(20) Barauskas, J.; Johnsson, M.; Joabsson, F.; Tiberg, F. Cubic Phase Nanoparticles (Cubosome): Principles for Controlling Size, Structure, and Stability. *Langmuir* **2005**, *21*, 2569−2577.
(21) Wörle, G.; Siekmann, B.; Koch, M. H. J.; Bunjes, H. Transformation of Vesicular into Cubic Nanoparticles by Autoclaving of Aqueous Monoolein/poloxamer Dispersions. *Eur. J. Pharm. Sci.* **2006**, *27*, 44−53.
(22) Israelachvili, J. N. *Intermolecular and Surface Forces*, revised third ed.; Academic Press: New York, 2011.
(23) Kulkarni, C. V.; Wachter, W.; Iglesias-Salto, G.; Engelskirchen, S.; Ahualli, S. Monoolein: A Magic Lipid? *Phys. Chem. Chem. Phys.* **2011**, *13*, 3004−3021.
(24) Yaghmur, A.; de Campo, L.; Sagalowicz, L.; Leser, M. E.; Glatter, O. Emulsified Microemulsions and Oil-Containing Liquid Crystalline Phases. *Langmuir* **2005**, *21*, 569−577.
(25) Fong, C.; Le, T.; Drummond, C. J. Lyotropic Liquid Crystal Engineering−ordered Nanostructured Small Molecule Amphiphile Self-Assembly Materials by Design. *Chem. Soc. Rev.* **2012**, *41*, 1297−1322.
(26) Mezzenga, R.; Grigorov, M.; Zhang, Z.; Servais, C.; Sagalowicz, L.; Romoscanu, A. I.; Khanna, V.; Meyer, C. Polysaccharide-Induced Order-to-Order Transitions in Lyotropic Liquid Crystals. *Langmuir* **2005**, *21*, 6165−6169.
(27) Klibanov, A. L.; Maruyama, K.; Torchilin, V. P.; Huang, L. Amphipathic Polyethyleneglycols Effectively Prolong the Circulation Time of Liposomes. *FEBS Lett.* **1990**, *268*, 235−237.
(28) Svensson, O.; Thuresson, K.; Arnebrant, T. Interactions between Drug Delivery Particles and Mucin in Solution and at Interfaces. *Langmuir* **2008**, *24*, 2573−2579.
(29) Boyd, B. Characterisation of Drug Release from Cubosomes Using the Pressure Ultrafiltration Method. *Int. J. Pharm.* **2003**, *260*, 239−247.
(30) Drescher, D.; Orts-Gil, G.; Laube, G.; Natte, K.; Veh, R. W.; Österle, W.; Kneipp, J. Toxicity of Amorphous Silica Nanoparticles on Eukaryotic Cell Model Is Determined by Particle Agglomeration and Serum Protein Adsorption Effects. *Anal. Bioanal. Chem.* **2011**, *400*, 1367−1373.
(31) Xia, T.; Kovochich, M.; Liong, M.; Mädler, L.; Gilbert, B.; Shi, H.; Yeh, J. I.; Zink, J. I.; Nel, A. E. Comparison of the Mechanism of Toxicity of Zinc Oxide and Cerium Oxide Nanoparticles Based on Dissolution and Oxidative Stress Properties. *ACS Nano* **2008**, *2*, 2121−2134.
(32) Serpe, L.; Catalano, M. G.; Cavalli, R.; Ugazio, E.; Bosco, O.; Canaparo, R.; Muntoni, E.; Frairia, R.; Gasco, M. R.; Eandi, M.; Zara, G. P. Cytotoxicity of Anticancer Drugs Incorporated in Solid Lipid Nanoparticles on HT-29 Colorectal Cancer Cell Line. *Eur. J. Pharm. Biopharm.* **2004**, *58*, 673−680.
(33) Zhang, Z.; Feng, S.-S. The Drug Encapsulation Efficiency, in Vitro Drug Release, Cellular Uptake and Cytotoxicity of Paclitaxel-Loaded Poly(lactide)−tocopheryl Polyethylene Glycol Succinate Nanoparticles. *Biomaterials* **2006**, *27*, 4025−4033.
(34) Aryal, S.; Jack Hu, C.-M.; Fu, V.; Zhang, L. Nanoparticle Drug Delivery Enhances the Cytotoxicity of Hydrophobic−hydrophilic Drug Conjugates. *J. Mater. Chem.* **2012**, *22*, 994.